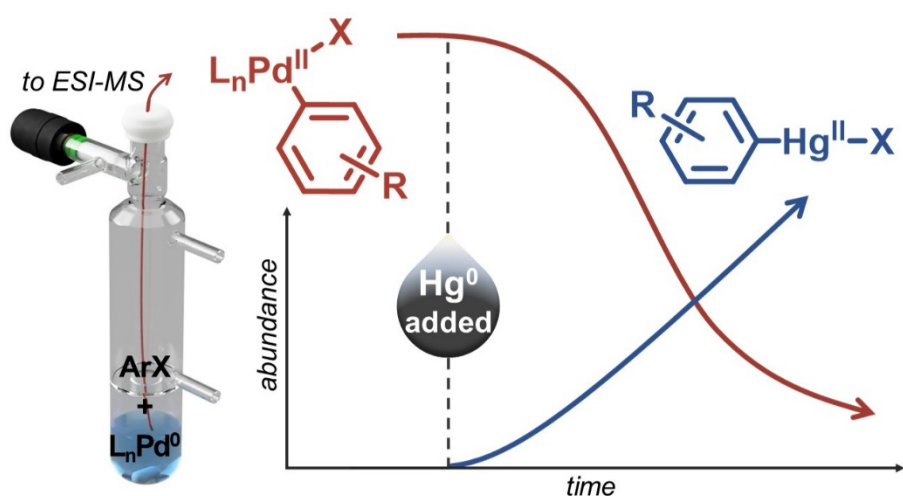# The poisonous truth about the mercury drop test: the effect of elemental mercury on Pd(0) and Pd(II)ArX intermediates

Ian C. Chagunda, Tiago Fisher, Makenna Schierling, J. Scott McIndoe*

Department of Chemistry, University of Victoria,

PO Box 1700 STN CSC, Victoria, BC V8W 2Y2, Canada.

Tel: +1 (250) 721-7181; E-mail: mcindoe@uvic.ca; Website: https://web.uvic.ca/~mcindoe/

Abstract

The mercury drop test is a widely used method for distinguishing between homogeneous and heterogeneous catalysis in organometallic systems. However, recent research has highlighted the limitations of this test due to the intrinsic reactivity of some organometallic compounds towards elemental mercury. In this study, we used real-time mass spectrometry with charge-tagged substrates to investigate the effect of elemental mercury on L_nPd^0 and $Pd^{II}ArX$ intermediates common in palladium-catalysed cross-coupling reactions. Our findings demonstrate that mercury can interact with both species through redox-transmetallation and amalgamation processes, leading to a decrease in catalytic activity. This result further calls into question the fundamental assumption of mercury selectivity towards heterogeneous catalytic species. These results highlight the importance of careful consideration of the results the mercury drop test provides and encourages further research to gain a more comprehensive understanding of catalyst poisoning mechanisms.

Keywords

mercury drop test, homogeneous catalysis, heterogeneous catalysis, catalyst poisoning reaction mechanisms, Pd complexes, real-time mass spectrometry.

Introduction

Palladium-catalysed cross-coupling (PdCC) is a powerful tool in modern synthetic chemistry.[1] This class of reactions has had a huge impact on the way in which chemists think about building fine chemicals, with innovative applications of palladium cross-coupling garnering new synthetic approaches to natural products,[2,3] pharmaceuticals,[4–6] and organic materials.[7,8] These reactions can be classified as either homogeneous or heterogeneous, depending on the nature of the palladium catalyst.

Recent research has challenged the traditional classification of catalysts into homogeneous and heterogeneous domains, as a more complex picture of complementary catalysis from multiple types of catalytic sites has emerged.[9–12] Homogeneous catalysts are defined to have a single type of active site, existing in the same phase as the reactants. These catalysts' reactivity and selectivity are highly dependent on their auxiliary ligands.[13–15] In contrast, a heterogeneous catalyst can have multiple types of active sites on metallic surfaces. The nature of the active site can be ambiguous as illustrated by literature supporting both soluble molecular and nanoparticle catalysts, as well as truly heterogeneous insoluble palladium catalysts.[16–18]

Since most significant catalytic properties including activity, selectivity, stability, and lifetime are affected differently for these two classes of catalysts, it is crucial to differentiate between true homogeneous catalysis and heterogeneous catalysis. Notably, a variety of industrial processes, such as efficient catalyst recovery, rely on the knowledge of the catalyst's identity. [19,20] However, accurately identifying whether a system involves metal-complex homogeneous catalysis or metal-particle heterogeneous catalysis is a difficult issue that has generated a lot of debate in the literature.[21–23]

Various tests have been used to determine the nature of active catalysts, but they are subject to limitations that can affect their accuracy and usefulness. These include physical separation methods such as filtration and centrifugation, where a comparison of reactivity of the filtrate and residue is used to discern the nature of active catalytic species.[20,21,24] Such tests are subject to errors due to difficulty in quantitative separation, and heterogeneous species continuing to grow in the filtrate.[20] Light scattering experiments are also used to detect metal particles, though this provides limited information about their catalytic relevance,[21] and while transmission electron microscopy (TEM) allows nanocluster visualization, it is still in its infancy for kinetic analysis due to limited instrument resources and high costs.[25]

Tests with high selectivity for homogeneous or heterogeneous species have been developed to modify and monitor catalytic kinetics, but their practical limitations make them challenging to use. Poisoning experiments, such as quantitative ligand poisoning using CS_2 or triphenylphosphine (PPh$_3$), can distinguish between heterogeneous and homogeneous catalysis by calculating the stoichiometry of ligand required to halt catalytic activity.[26–28] Similarly, Crabtree's test uses dibenzo[*a,e*]cyclooctatetraene (DCT) to selectively inhibit catalytic activity in homogeneous species.[29] However, due to challenging reaction conditions such as the necessity to be carried out at low temperatures for CS_2 (and hence extended reaction times), and in the case of the DCT synthetic technique, their poor yields, these tests are not widely utilized.[30]

The mercury drop test is the most widely used poisoning test for distinguishing between homogeneous and heterogeneous catalysis.[31–34] This test is based on the simple assumption that elemental mercury, Hg^0, will amalgamate with metal heterogeneous catalysts, M^0, considerably reducing or eliminating their catalytic activity, while homogeneous metals of higher oxidation states bearing protective ligands, L_nMX, will be left unaffected (Scheme 1). If

a sufficient amount of mercury is added to a catalytic reaction, a decrease in catalytic activity is evidence of a heterogeneous catalyst, while a negative mercury test implies that the reaction is homogenous.[35] A review of over 400 papers published between 2015 and 2018 found that in 68% of the cases, the mercury test was the only technique used for distinguishing between homogeneous and heterogeneous catalysis mechanisms.[36]
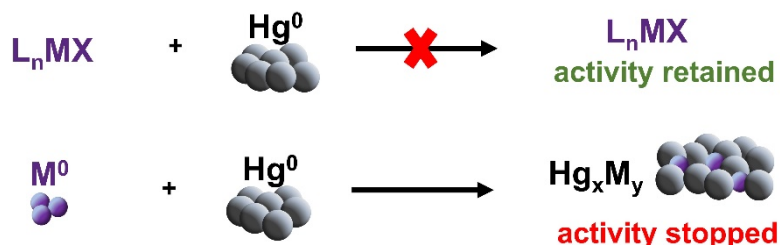
Scheme 1: General principle of the mercury drop test for organometallic catalysis.

The accuracy of this test has been called into question due to limitations in reaction conditions and the reactivity of some organometallic compounds towards mercury. Whitesides and co-authors warned about the these drawbacks in the 1980s, pointing to the possibility of interactions between mercury and some organometallic compounds.[37] Subsequent investigations have since confirmed susceptibility of the test to inaccuracies due to the intrinsic reactivity of a number of organometallic compounds of Pd, Pt, Rh, and other metals toward elemental mercury.[22,38–42] Furthermore, reaction conditions such as stoichiometry, stir rate, and temperature can significantly impact the test's sensitivity, further casting doubt on the validity of some results.[36] Given these limitations, the effectiveness of the mercury drop test in accurately distinguishing between homogeneous and heterogeneous catalysis remains contentious.

We applied electrospray mass spectrometry (ESI-MS) to monitor the effects of the mercury drop test on a simple palladium-catalysed cross-coupling reaction, which revealed important insights into reaction intermediates. Specifically, we aimed to interrogate how mercury interacts with the first two intermediates in the reaction cycle, namely the Pd^0 species formed after catalyst activation of precatalyst with a ligand, and the Pd^{II} species formed after oxidative addition of ArX. The intermediates further along in the cycle cannot be as unambiguously examined, as upon addition of the cross-coupling partner the cycle can turn over and the resulting system is complicated by the simultaneous presence of multiple intermediates. Nonetheless, real-time monitoring of these reactions enabled us to identify significant catalytic and mercuric species, shedding light on the reactivity of these entities.

Results and Discussion

ESI-MS is a powerful and sensitive technique for analyzing organometallic reactions,[43–49] and has previously been combined with pressurized sample infusion (PSI) to elucidate mechanisms and identify catalytically relevant species.[50–53] By using charge-tagged ligands and substrates, neutral catalytic species can be detected that would typically go undetected by MS. This method has been widely used for kinetic analysis,[54] with similar methodology applied herein to study a palladium cross-coupling reaction.

Effects of mercury on catalyst activation Pd⁰ species

Recent research has provided evidence of interactions between mercury and palladium precatalysts in catalyzed reactions. While many have used the inhibition of catalysis upon the addition of mercury prior to catalyst activation as evidence for the involvement of heterogeneous species,[55,56] Gorunova and co-authors suggested that this could indicate reactivity with the homogeneous precatalyst.[39] Work by Chernychev and co-authors provided evidence for such interactions, demonstrating how the precatalyst tris(dibenzylideneacetone)dipalladium(0), $Pd_2(dba)_3$, reacted with Hg^0 to form free dba and other organomercuric species, leading to the near-complete disappearance of dissolved palladium within 30 minutes.[36] In light of these findings, our investigations began with monitoring the *in-situ* activation of Pd precatalyst, and the effects of mercury thereupon.

We employed $Pd_2(dba)_3$, a commonly used source of Pd^0, along with a charge-tagged triphenylphosphine derivative $[PPN]^+[PPh_2(m\text{-}C_6H_4SO_3)]^-$, [PPN][1] (PPN = bis(triphenylphosphino)iminium cation), to investigate the effects of elemental mercury on catalyst activation.[57,58] As shown in Figure 1, we used PSI-ESI-MS techniques to monitor a solution of [PPN][1] in negative ion mode on a Waters Synapt G2-S*i* mass spectrometer until a steady signal was obtained. Subsequent syringe addition of $Pd_2(dba)_3$ to the solution of [PPN][1] at 5 minutes resulted in catalyst activation, with rapid formation of mono- and bisligated Pd^0 species $[Pd(1)_n(dba)_m]^{n-}$, where n = 1-2, and m = 0-1. The speciation is similar to what has been previously reported (see Figure S4 for detailed MS characterisation).[59] These activated catalyst resting states remained stable in solution for at least 25 minutes. The formation of $[Pd(1)_n(dba)_m]^{n-}$ occurred in a time frame faster than solution could move from reaction flask to MS, which has an delay of approximately 25 s.[54] We are therefore limited to stating that $t_{1/2}$ < ~10 s.
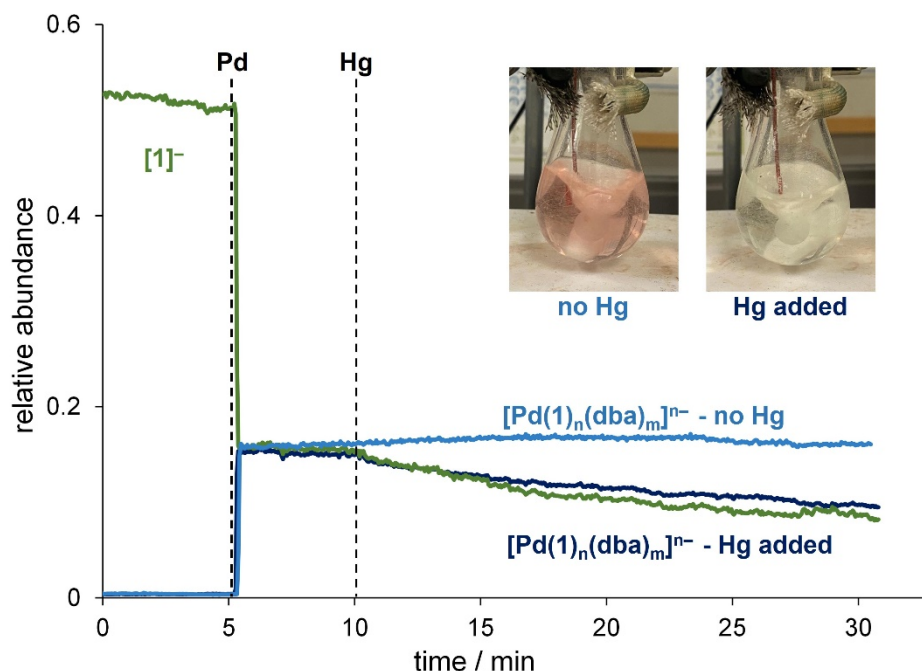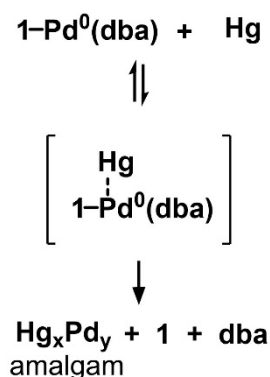

Figure 1: PSI-ESI(−)-MS reaction monitoring showing the effects of Hg addition on catalyst activation. A drop in relative abundance of catalyst resting state $[Pd(1)_n(dba)_m]^{n-}$ (dark blue) and $[1]^-$ (green) is observed upon Hg addition (10 min). Control experiment with no Hg addition shown in light blue. **Inset**: Solution colour change observed upon mercury addition.

Upon adding Hg^0 into the reaction (Figure 1 at 10 minutes), a drop in the relative abundance of the catalyst resting state $[Pd(\mathbf{1})_n(dba)_m]^{n-}$ was initiated. After a 40-minute examination of the reaction solution, a colour change from light purple to yellow was observed, indicating the release of free dba into solution (Figure 1, inset). No species with characteristic mercury isotope patterns were detected during this reaction in MS negative mode, suggesting that Pd^0 nanoparticles and/or Hg_xPd_y amalgamation as the likely destination of the Pd. The favourable thermodynamics of amalgamation with Pd^0 species further supports this observation ($PdHg_4$ ΔG_{298} = −84.0 kJ mol^{-1}).[60] Scheme 2 depicts a proposed route for this catalyst deactivation. Although the precise mechanism for this catalyst deactivation is unclear, it may involve the initial adsorption of Pd^0 intermediates onto the mercury surface, resulting in the formation of unstable L_nPd_y-Hg_x intermediates. In the case of $[Pd(\mathbf{1})_n(dba)_m]^{n-}$ where n = 2, a ligand dissociation may first occur resulting in an electron-deficient Pd centre that is more readily adsorbed. Subsequent ligand dissociation would form solvated ligands and Hg_xPd_y amalgam.

$$\mathbf{1}–Pd^0(dba) \;+\; Hg$$

$$\Updownarrow$$

$$\left[\begin{array}{c} Hg \\ \vdots \\ \mathbf{1}–Pd^0(dba) \end{array} \right]$$

$$\downarrow$$

$$Hg_xPd_y \;+\; \mathbf{1} \;+\; dba$$
amalgam

Scheme 2: Proposed pathway for the formation of Hg_xPd_y
amalgam from Pd^0 catalyst activation intermediates.

Contrary to our initial hypothesis, the addition of mercury to $[Pd(\mathbf{1})_n(dba)_m]^{n-}$ resulted in a decrease in the relative abundance of both $[Pd(\mathbf{1})_n(dba)_m]^{n-}$ and $[\mathbf{1}]^-$. This was accompanied by an increase in the relative abundance of the oxide of **1** due to phosphine oxidation. Phosphine ligand oxidation is a known palladium catalysis phenomenon that can lead to catalyst deactivation and termination of the reaction.[61,62] We have previously shown how the presence of dioxygen in solution results in the palladium-catalyzed oxidation of triphenylphosphine.[63] We suspected that introduction of uncontrolled amounts of air at the addition of mercury likely accelerated the phosphine oxidation in $[Pd(\mathbf{1})_n(dba)_m]^{n-}$, leading to the observed decrease in the relative abundance of $[\mathbf{1}]^-$. Our investigation revealed that the summed intensities of the two species remained unchanged after the addition of mercury, indicating an increase in the abundance of the oxide of **1** and a decrease in the relative abundance of $[\mathbf{1}]^-$ due to phosphine oxidation. Refer to Figure S5 for more details.

To test the impact of the presence of air, we repeated the catalyst activation experiment detailed in Figure 1, but with 1 mL of air injected into the reaction flask headspace at 20 minutes, instead of mercury. We observed only a minimal increase in phosphine oxide formation in these experiments. Notably, the colour change observed with mercury addition was not observed in these control experiments; the purple colour remaining even after 24 hours of stirring the sealed flask. These results suggest that while some of the phosphine oxidation seen in Figure 1 could be attributed to air contamination during mercury addition, the extensive catalyst decomposition is the result of the interaction of metallic mercury with Pd^0 intermediates. These findings demonstrate the limitations of monodentate phosphine ligands, which are commonly thought to be effective protectors.[35] Despite their reputation and wide use, our results show that triphenylphosphine and similar monodentate phosphine

ligands are not effective at protecting homogeneous Pd^0 intermediates in mercury testing under these conditions. After observing decomposition of Pd^0 catalyst activation intermediates, we shifted our attention towards the product of the oxidative addition step to investigate the reactivity of mercury with palladium in the +2 oxidation state.

Effects of mercury on oxidative addition Pd^{II} species.

We monitored the reactivity of mercury with the Pd^{II} intermediates produced by oxidative addition and protected by monodentate phosphine ligands. After catalyst activation had reached a steady state, an excess of iodobenzene, PhI, was added, causing $[Pd(\mathbf{1})_n(dba)_m]^{n-}$ to be consumed and primarily replaced by the Pd^{II} species $[Pd(\mathbf{1})(Ph)(I)]^-$ (Figure 2, 10-30 min). Oxidative addition occurred at a significantly slower rate than catalyst activation, likely due to the requirement of dba decoordination prior to the reaction occurring.[58] For the first 10 minutes until equilibrium was reached, the disappearance of $[Pd(\mathbf{1})_n(dba)_m]^{n-}$ produced a linear plot of the natural log of its intensity vs. time, with $t_{1/2}$ = 3.3 minutes, indicating first order kinetics. We observed the appearance of I^-, likely resulting from a dissociative equilibrium between $[Pd(\mathbf{1})(Ph)(I)]^-$ and unobserved $Pd(\mathbf{1})(Ph)$. In polar solvents, $L_nPd(Ar)(X)$ complexes feature cationic $[L_nPd(Ar)]^+$ species,[64] making the halide dissociation product $Pd(\mathbf{1})(Ph)$ zwitterionic. Additionally, we observed the anionic bisligated $[Pd(\mathbf{1})_2(Ph)]^-$ in much lower abundance following a similar kinetic profile, indicating its involvement in halide dissociation equilibria.
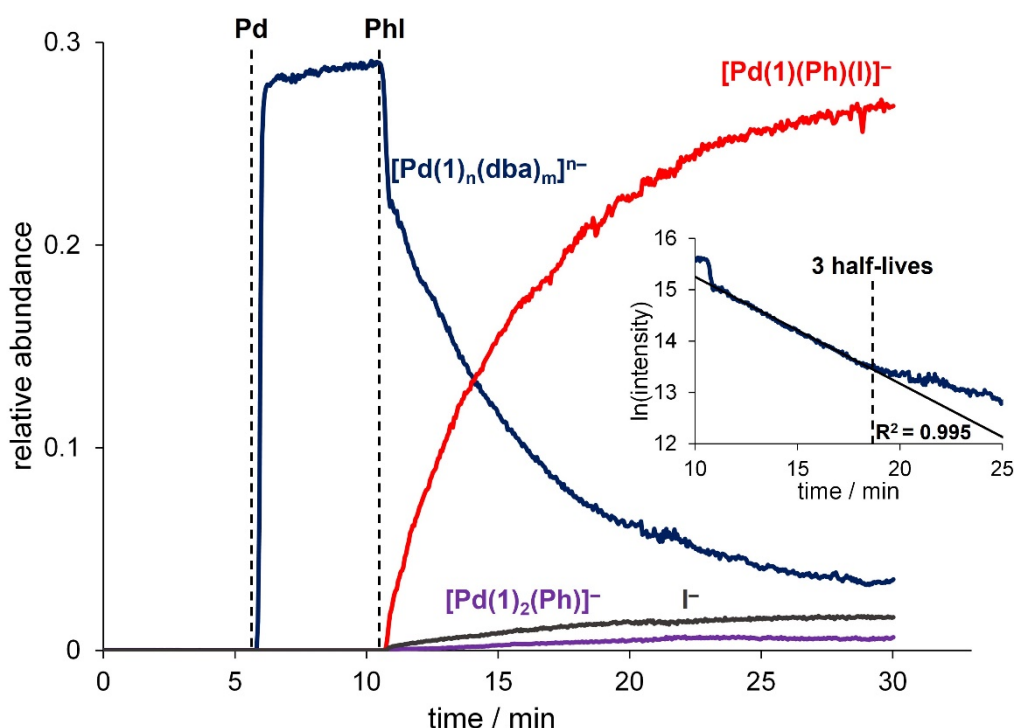

Figure 2: PSI-ESI(–)-MS reaction monitoring of the oxidative addition of iodobenzene to $[Pd(\mathbf{1})_n(dba)_m]^{n-}$, where n = 1-2, m = 0-1 over 30 minutes. Inset: natural log of intensity of $[Pd(\mathbf{1})_n(dba)_m]^{n-}$ over time showing pseudo-first-order kinetics up to 3 half-lives.

Elemental mercury was added to the reaction after the abundance of the oxidation addition product had stabilized (Figure 3, 20 min), resulting in significant changes in the reaction profiles of multiple species. Firstly, the consumption of the catalyst resting state $[Pd(\mathbf{1})_n(dba)_m]^{n-}$ was accelerated as seen in Figure 1. There was no recovery in the abundance

of $[Pd(\mathbf{1})_n(dba)_m]^{n-}$, suggesting that the principal destination of the palladium is to Pd^0 nanoparticles and amalgamation. Additionally, we observed that mercury increases the amount of ligand $[\mathbf{1}]^-$ in solution. The reappearance of $[\mathbf{1}]^-$ closely tracks with the disappearance of $[Pd(\mathbf{1})Ph(I)]^-$, suggesting that the phosphine is decoordinated from the Pd^{II} intermediate during the reaction with Hg^0. We also observed an increase in the amount of $[Pd(\mathbf{1})_2Ph]^-$, which accounts for about two-thirds of the Ph-containing ions present after mercury addition. Furthermore, trace quantities of the organomercuric species $[Hg(I)_2Ph]^-$ (Figure 3 inset), as well as $[Pd(\mathbf{1})Ph_2(dba)]^-$ were also detected, accounting for some of the "missing" Ph-containing ions. It is important to note that the mass balance obtained by ESI-MS is not reliable due to differences in surface activities of the various ions in solution,[65] and these activities are not measurable due to the impracticalities of isolating the individual components.
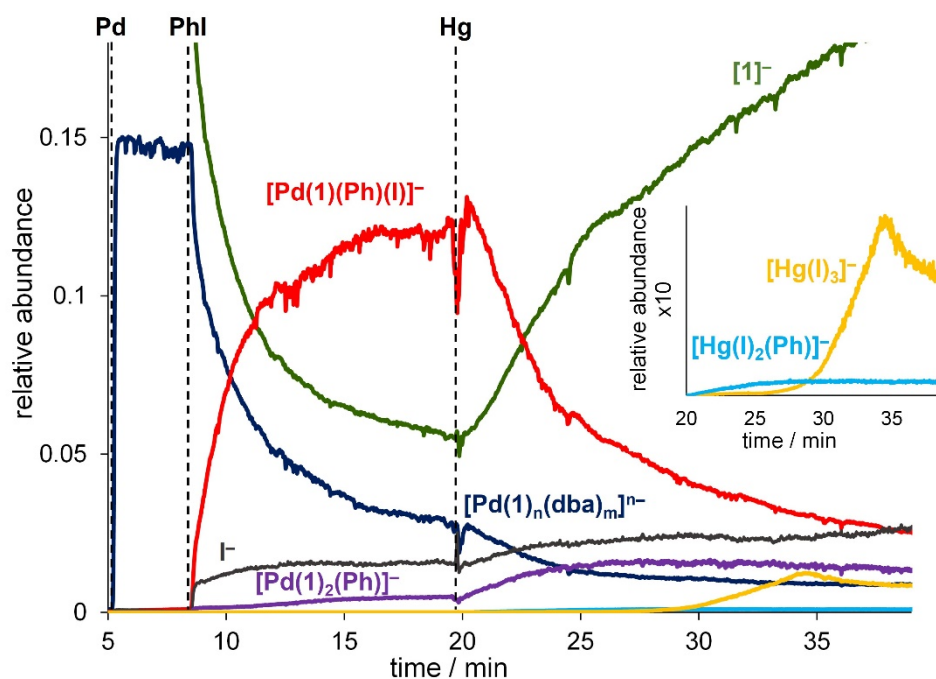

Figure 3: PSI-ESI(–)-MS reaction monitoring of the effects of Hg on the oxidative addition of iodobenzene to $[Pd(\mathbf{1})_n(dba)_m]^{n-}$, where n = 1-2, m = 0-1. Inset displays low abundance species with relative intensities multiplied by a factor of ten.

Studies have shown that both dissolved Hg^0 species and liquid mercury readily oxidize in aqueous media in the presence of halides.[66–68] We observed evidence of this oxidation occurring in methanol with the detection of $[HgI_3]^-$ 10 minutes after adding mercury. A proposed mechanism (see Scheme 3) involves the Pd^{II} intermediate adsorbing on metallic mercury, followed by reduction of Pd^{II} via electron transfer to Hg^0, and iodide transfer to form $[HgI]^+$ and $[Pd(\mathbf{1})(Ph)]^{2-}$. The resulting Pd^0 species follow similar pathways as outlined in Scheme 2, forming Hg_xPd_y amalgams. The increase in abundance of $[Pd(\mathbf{1})_2(Ph)]^-$ is likely due to iodide abstraction from $[Pd(\mathbf{1})(Ph)(I)]^-$ by $[HgI]^+$, with free phosphine $\mathbf{1}$ filling the vacant coordination site. These findings suggest that the oxidation of mercury by halides is a complex process with multiple steps.
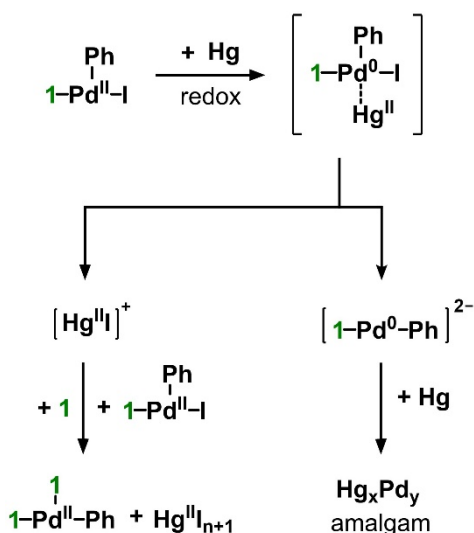
Scheme 3: Proposed pathways for the mercury redox decomposition of Pd^{II} oxidative addition intermediate forming mercuric iodide, $[Pd(\mathbf{1})_2Ph]^-$ and Hg_xPd_y amalgam.

We expected the abundance of iodide to decrease after the introduction of mercury due to the formation of the iodomercuric species. Surprisingly, we instead observed a steady increase in abundance of I^- before reaching steady state after several minutes. To better understand this phenomenon, we conducted tandem MS experiments on $[HgI_3]^-$, which revealed that iodide dissociation occurred at collision energies less than 2 V; ligand dissociation more typically occurs at >10 V (see Table S1). It is possible that this dissociation is occurring in the mass spectrometer under standard source conditions, leading to the observed increase in I^- abundance. According to the literature, the stability constants of $[HgI_3]^-$ and $[HgI_4]^{2-}$ are similar.[69] However $[HgI_4]^{2-}$ was absent in our experiments, likely due to the limited stability of polyanionic gas phase species, which when not stabilized by solvation are prone to loss of X^- or evaporation of an electron.[70] The flattening of the rate of iodide dissociation indicates equilibria being reached between $[HgI]^+$, HgI_2, $[HgI_3]^-$, and $[HgI_4]^{2-}$.

This formation of $[HgI_3]^-$ is likely due to redox iodide abstraction as shown in Scheme 3. In addition, we observed the formation of $[Hg(I)_2Ph]^-$ and trace amounts of $[Pd(\mathbf{1})(Ph)_2(dba)]^-$, suggesting transmetallation occurred between Hg^0 and Pd^{II}. Transmetallation involving organomercury compounds has been studied previously for its use in palladium-catalyzed cross-coupling reactions.[71–75] More recently, bis(ferrocenyl)mercury was used as a transmetallation partner to produce a range of ferrocene-containing molecules via palladium-catalyzed cross-coupling reactions with aryl, heteroaryl, acid halides, and alkynes.[76,77] All of these examples involve organomercuric reagents (R_2Hg or $RHgX$) in the Hg^{II} oxidation state. Given these findings, our next step was to investigate transmetallation with Hg^{II} species generated via *in-situ* oxidation of elemental mercury.

Investigation of Pd/Hg redox-transmetallation

A sulfonated analogue of iodobenzene $[PPN]^+[IC_6H_4CH_2SO_3]^-$, [PPN][**2**], was used to enable MS monitoring of possible transmetallation intermediates. When tetrakis(triphenylphosphine)palladium(0), $Pd(PPh_3)_4$, is added to a solution of [PPN][**2**], the expected Pd^{II} oxidative addition products $[(PPh_3)_mPd(I)(C_6H_4CH_2SO_3)]^-$ (m = 1-2) quickly formed. After the signal stabilized, liquid mercury was added, which resulted in the formation of the organomercuric species $[Hg(I)(C_6H_4CH_2SO_3)]^-$ via transmetallation (following pseudo-

zero order kinetics due to the excess of Hg present, see Figure 4). $[Hg(I)_2X]^-$ (X = I or Cl) was also detected approximately 5 minutes after mercury addition, an induction period presumably due to the requirement for preceding formation of $[HgI]^+$ and HgI_2 (see Figure S8 for detailed MS species characterisation).
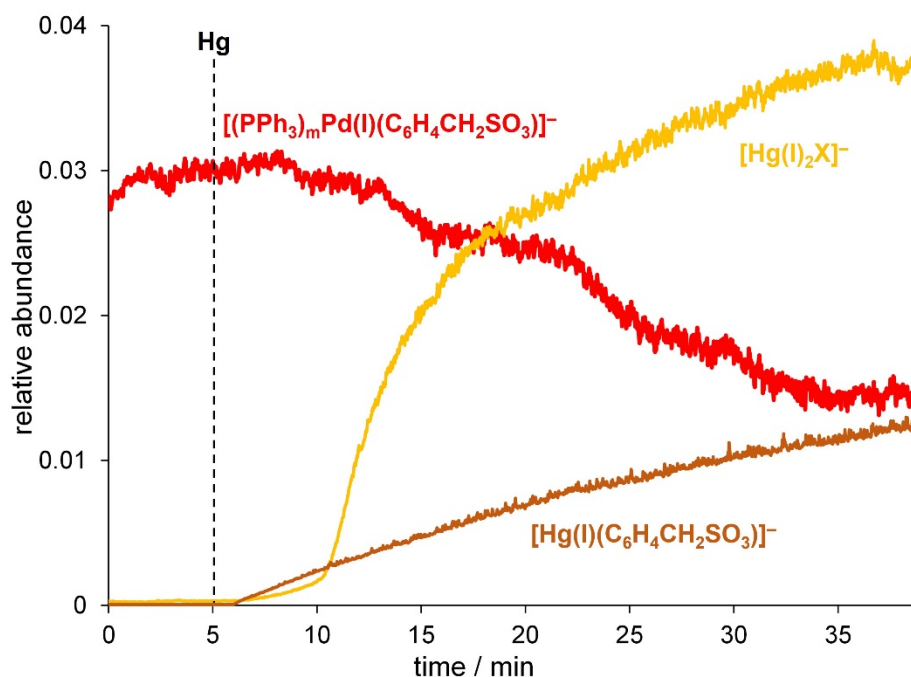

Figure 4: PSI-ESI(−)-MS reaction monitoring of the effects of Hg on the Pd^{II} oxidative addition intermediate $[(PPh_3)_mPd(I)(C_6H_4CH_2SO_3)]^-$, where m = 1-2. Pd/Hg transmetallation of substrate occurs with the immediate formation of $[Hg(I)(C_6H_4CH_2SO_3)]^-$, as well as $[Hg(I)_2X]^-$ (X = I or Cl).

Scheme 4 proposes a pathway for the transmetallation between organopalladium intermediates and elemental mercury. The reaction likely occurs via an inner-sphere mechanism mediated by activated iodide or aryl ligands forming bridged intermediates.[78] Following this, a ligand transfer to mercury occurs, with ligand coordination being thermodynamically favourable for less electronegative mercury. The exact nature of the ligand and electron transfer remains unresolved; it is unclear whether it is a concerted process involving both bridged ligands (as shown in Scheme 4.a) or if a more complex stepwise mechanism is involved. Other studies have discussed the formation of Pd-Hg-X intermediates, involving an initial insertion of mercury into a weakened Pd-X bond,[79–81] followed by an aryl ligand *cis*-migration to mercury (as shown in Scheme 4.b). Similar compounds with Pt-Hg bonds have been reported, suggesting that such a mechanism could be at play in this system.
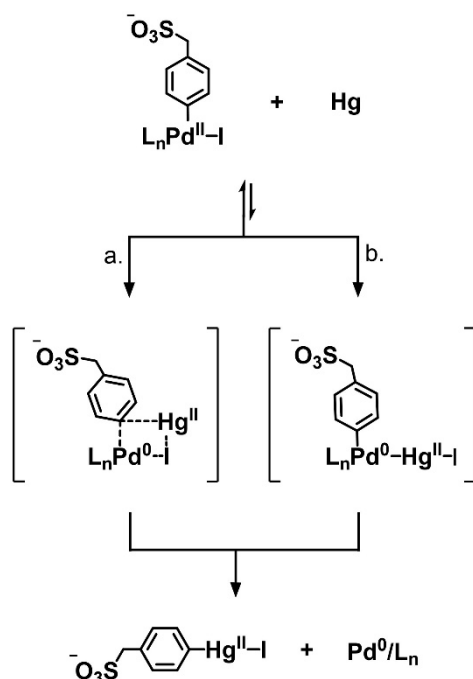
Scheme 4: Proposed pathway for Pd/Hg redox transmetallation forming $[Hg(I)(C_6H_4CH_2SO_3)]^-$, via **a**) iodide- and aryl-bridged intermediate, and **b**) insertion of Hg into a weakened Pd-I bond.

Control experiments were conducted to investigate the transmetallation product. Charge-tagged analogues of iodobenzene were used with liquid mercury added but no palladium. None of these analogues reacted, suggesting that the $[Hg(I)(C_6H_4CH_2SO_3)]^-$ ion is a redox-transmetallation product, rather than a simple a C–I bond insertion. To test for a possible cross-coupling product $[Ph(C_6H_4CH_2SO_3)]^-$, equimolar amounts of PhI and the charge-tagged analogue [**2**]$^-$ were added to the same reaction flask, but neither the expected reductive elimination product $[Ph(C_6H_4CH_2SO_3)]^-$ (*m/z* 247) nor the transmetallation intermediate $[(PPh_3)Pd(Ph)(C_6H_4CH_2SO_3)]^-$ (*m/z* 615) were observed.

Several factors may be responsible for preventing the reaction from occurring. Previous research has shown that electron-donating substituents on aryl iodides can hinder the reaction,[76] in addition to the presence of the anionic sulfonate group that may disfavor coordination to palladium due to electrostatic repulsion. Additionally, the bulky nature of the counterion, [PPN]$^+$, may also hinder the entry of organomercurials into the coordination sphere of palladium.

To gain a deeper understanding of the Pd^{II} and Hg^{II} transmetallation intermediates, fragmentation via collision-induced dissociation (CID) was used to generate product ions. We optimised the collision energies such that the abundance of precursor ions was reduced to 10% of their initial intensity, with the Pd^{II} precursor ion $[(PPh_3)Pd(I)(C_6H_4CH_2SO_3)]^-$, requiring 18 V and Hg^{II} requiring 15 V (Figure 5). At a collision energy of 10 V for the Pd^{II} ion, we detected a neutral loss of *m/z* 262.1 (PPh$_3$). PPh$_3$ readily dissociates from palladium as an L-type ligand through a simple ligand dissociation, hence the lower voltage. In contrast, X-type ligands require more energy for homolytic dissociation due to the necessity of radical formation.[82] This low energy PPh$_3$ dissociation was also observed for the bisligated $[(PPh_3)_2Pd(I)(C_6H_4CH_2SO_3)]^-$ ion at collision energies of 1 V (see Table S1). Moreover, we observed a product ion at *m/z* 296.9, which was assigned to the reductive elimination of the charge-tagged aryl halide $[IC_6H_4CH_2SO_3]^-$ (Figure 5.a).

The Hg^{II} transmetallation intermediate showed different unimolecular decomposition pathways, with the charge-tagged aryl fragment [C$_6$H$_4$CH$_2$SO$_3$]$^-$ (*m/z* 170.0) having the greatest relative abundance (Figure 5.b). This product ion, as well as I$^-$ (*m/z* 126.9), results from homolytic cleavage of the X-type ligands. This CID reaction pathway was not observed for the Pd^{II} precursor ion, which has a square planar geometry that makes reductive elimination a more favorable pathway. The linear geometry of the Hg^{II} intermediate, on the other hand, disfavors reductive elimination, and hence the homolytic cleavage product ions are most abundant for Hg^{II}.
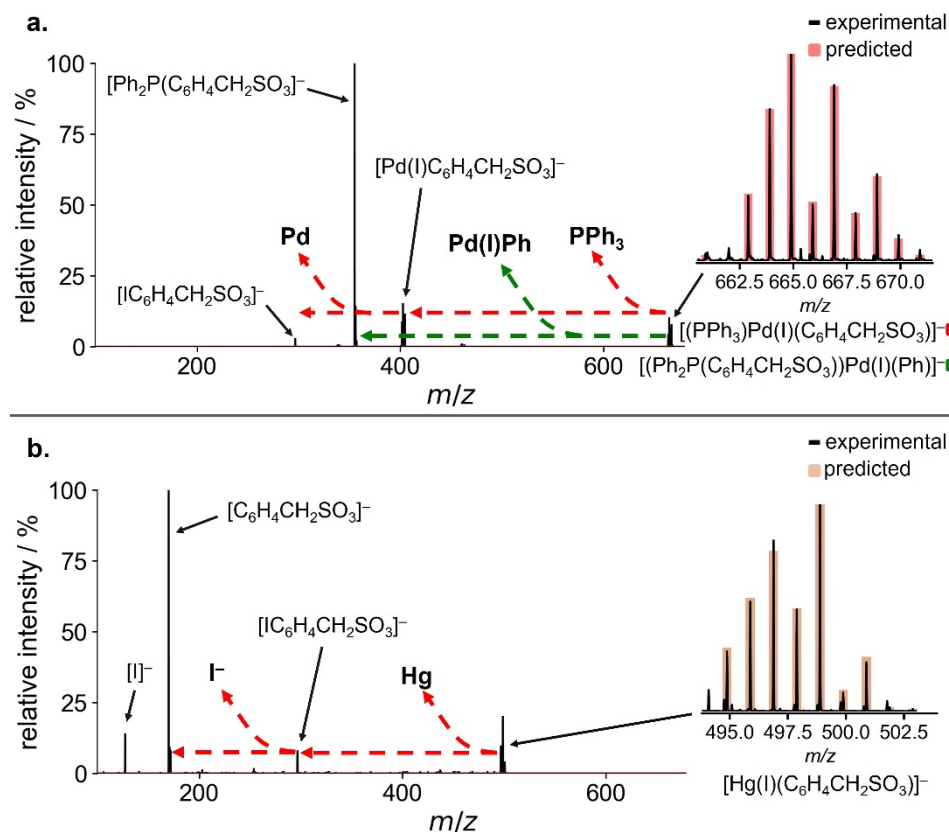

Figure 5: **a;** ESI(−)-MS/MS (CE = 18 V) of [(PPh$_3$)Pd(I)(C$_6$H$_4$CH$_2$SO$_3$)]$^-$ at *m/z* 664.9, showing product ions [Pd(I)(C$_6$H$_4$CH$_2$SO$_3$)]$^-$ (*m/z* 402.8), [IC$_6$H$_4$CH$_2$SO$_3$]$^-$ (*m/z* 296.9), and phosphine scrambling product ion [Ph$_2$P(C$_6$H$_4$CH$_2$SO$_3$)]$^-$ (*m/z* 355.1). **b;** ESI(−)-MS/MS (CE = 15 V) of [Hg(I)(C$_6$H$_4$CH$_2$SO$_3$)]$^-$ at *m/z* 498.9, showing product ions [IC$_6$H$_4$CH$_2$SO$_3$]$^-$ (*m/z* 296.9), [C$_6$H$_4$CH$_2$SO$_3$]$^-$ (*m/z* 170.0), and I$^-$ (*m/z* 126.9). **Insets**; the predicted isotope pattern (bars) overlaid on the experimental mass spectrum (lines) of [Hg(I)(C$_6$H$_4$CH$_2$SO$_3$)]$^-$ and [(PPh$_3$)Pd(I)(C$_6$H$_4$CH$_2$SO$_3$)]$^-$.

Detection of the Pd^{II} product ion [Ph$_2$P(C$_6$H$_4$CH$_2$SO$_3$)]$^-$ (*m/z* 355.1), indicates the occurrence of intramolecular aryl-phosphine scrambling (see Figure 5.a, green). This phenomenon, in which aryl groups bound to palladium and phosphorus exchange positions, is a known side reaction in palladium-catalyzed cross-coupling reactions, often leading to undesired scrambled side products and catalyst deactivation.[83–86] Our results suggest that the scrambling process is facile,[51,87] and can be easily initiated under energetic CID conditions. We also observed evidence for aryl-phosphine scrambling in full scan ESI(−)-MS experiments, indicating that it occurs even in the absence of high energy CID conditions (see Figure S9).

A proposed mechanism for the solution-phase aryl-phosphine scrambling pathway is shown in Scheme 5. This involves the reductive elimination of a phosphonium salt intermediate, a known by-product in cross-coupling reactions.[88,89] This intermediate undergoes an oxidative addition to produce the aryl-phosphine scrambling Pd species with a new P-C bond,[86,90] which

further fragments by CID to produce the detected product ion $[Ph_2P(C_6H_4CH_2SO_3)]^-$. These findings provide insight into the characteristics of Pd^{II} and Hg^{II} transmetallation intermediates and can be used to diagnose substrate binding strength and composition.[91–94]
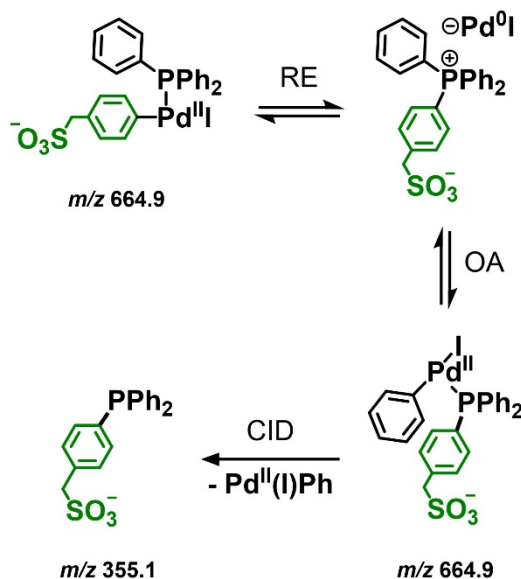
Scheme 5: Proposed mechanism of aryl-phosphine scrambling showing reductive elimination (RE) and oxidative addition (OA) resulting in new P-C bond formation and product ion $[Ph_2P(C_6H_4CH_2SO_3)]^-$ (*m/z* 355.1) following collision induced dissociation (CID).

Conclusions

Real-time mass spectrometric analysis of the effects of mercury on a model palladium catalysed cross-coupling reaction has revealed the limitations of the mercury drop test. Our findings indicate that elemental mercury can interact with both L_nPd^0 and $Pd^{II}ArX$ intermediates, leading to the formation of inactive complexes and inhibition of catalytic activity. Elemental mercury accelerated the consumption of $Pd^{0/II}$ homogeneous catalyst resting states, resulting in the formation of organomercuric ions, mercuric halides, and catalyst deactivation through Pd nanoparticles and amalgamation. Additionally, we observed transmetallation between organopalladium intermediates and elemental mercury. We postulate that the ligand transfer occurs through a thermodynamically favorable inner-sphere redox-transmetallation process, although the exact nature of ligand and electron transfer remains unresolved.

Our results show that the assumption that protective ligands, such as triphenylphosphine, prevent elemental mercury from interacting with palladium complexes of elevated oxidation states, is questionable. The minimal protective properties of monodentate phosphines are likely due to their easy dissociation from the metal complex. Although the palladium-catalysed cross-coupling discussed herein is a good representation of a common organometallic catalysis system, further investigations of other systems is crucial to understand the reactivity of elemental mercury and its catalyst poisoning mechanisms more comprehensively. Therefore, we intend to use our methodology in subsequent publications to further explore interactions of mercury with different metal catalysts and ligand systems.

Despite its shortcomings, the mercury drop test has long been used as a quick and easy method for determining whether a catalytic reaction is homogeneous or heterogeneous.

However, this test has limitations that have recently been highlighted by other researchers. For example, the reactivity of mercury with palladium in other ligand systems, such as *N*-heterocyclic carbenes (NHCs), and in *C,N*- and *C,P*-palladacycle systems, has raised concerns about the accuracy of the test.[36,38–40] These studies underscore the need for more rigorous testing methods that take into account the complex nature of organometallic catalysis. It is therefore crucial to raise awareness about the limitations of the mercury drop test and promote the use of alternative methods. Our study contributes to this effort and highlights real-time mass spectrometric monitoring techniques as a foundation for further research on catalyst poisoning mechanisms. We hope that our contributions will encourage wider recognition of the limitations of the mercury drop test and stimulate the development of alternative methods for the analysis of organometallic catalytic systems.

Acknowledgements

References

(1) Johansson Seechurn, C. C. C.; Kitching, M. O.; Colacot, T. J.; Snieckus, V. Palladium-Catalyzed Cross-Coupling: A Historical Contextual Perspective to the 2010 Nobel Prize. *Angew. Chem. Int. Ed.* **2012**, *51* (21), 5062–5085. https://doi.org/10.1002/anie.201107017.

(2) Touré, B. B.; Hall, D. G. Natural Product Synthesis Using Multicomponent Reaction Strategies. *Chem. Rev.* **2009**, *109* (9), 4439–4486. https://doi.org/10.1021/cr800296p.

(3) Wang, D.; Gao, S. Sonogashira Coupling in Natural Product Synthesis. *Org. Chem. Front.* **2014**, *1* (5), 556–566. https://doi.org/10.1039/C3QO00086A.

(4) Torborg, C.; Beller, M. Recent Applications of Palladium-Catalyzed Coupling Reactions in the Pharmaceutical, Agrochemical, and Fine Chemical Industries. *Adv. Synth. Catal.* **2009**, *351* (18), 3027–3043. https://doi.org/10.1002/adsc.200900587.

(5) Agasti, S.; Mondal, B.; Achar, T. K.; Sinha, S. K.; Sarala Suseelan, A.; Szabo, K. J.; Schoenebeck, F.; Maiti, D. Orthogonal Selectivity in C–H Olefination: Synthesis of Branched Vinylarene with Unactivated Aliphatic Substitution. *ACS Catal.* **2019**, *9* (10), 9606–9613. https://doi.org/10.1021/acscatal.9b03019.

(6) Rayadurgam, J.; Sana, S.; Sasikumar, M.; Gu, Q. Palladium Catalyzed C–C and C–N Bond Forming Reactions: An Update on the Synthesis of Pharmaceuticals from 2015–2020. *Org. Chem. Front.* **2021**, *8* (2), 384–414. https://doi.org/10.1039/D0QO01146K.

(7) Messina, C.; Douglas, L. Z.; Liu, J. T.; Forgione, P. Successive Pd-Catalyzed Decarboxylative Cross-Couplings for the Modular Synthesis of Non-Symmetric Di-Aryl-Substituted Thiophenes. *Eur. J. Org. Chem.* **2020**, *2020* (32), 5182–5191. https://doi.org/10.1002/ejoc.202000780.

(8) Rohand, T.; Qin, W.; Boens, N.; Dehaen, W. Palladium-Catalyzed Coupling Reactions for the Functionalization of BODIPY Dyes with Fluorescence Spanning the Visible Spectrum. *Eur. J. Org. Chem.* **2006**, *2006* (20), 4658–4663. https://doi.org/10.1002/ejoc.200600531.

(9) Appleby, K. M.; Dzotsi, E.; Scott, N. W. J.; Dexin, G.; Jeddi, N.; Whitwood, A. C.; Pridmore, N. E.; Hart, S.; Duckett, S. B.; Fairlamb, I. J. S. Bridging the Gap from Mononuclear PdII Precatalysts to Pd Nanoparticles: Identification of Intermediate Linear [Pd3(XPh3)4]2+ Clusters as Catalytic Species for Suzuki–Miyaura Couplings (X = P, As). *Organometallics* **2021**, *40* (21), 3560–3570. https://doi.org/10.1021/acs.organomet.1c00452.

(10) Scott, N. W. J.; Ford, M. J.; Jeddi, N.; Eyles, A.; Simon, L.; Whitwood, A. C.; Tanner, T.; Willans, C. E.; Fairlamb, I. J. S. A Dichotomy in Cross-Coupling Site Selectivity in a Dihalogenated Heteroarene: Influence of Mononuclear Pd, Pd Clusters, and Pd Nanoparticles—the Case for Exploiting Pd Catalyst Speciation. *J. Am. Chem. Soc.* **2021**, *143* (25), 9682–9693. https://doi.org/10.1021/jacs.1c05294.

(11) Ananikov, V. P.; Beletskaya, I. P. Toward the Ideal Catalyst: From Atomic Centers to a "Cocktail" of Catalysts. *Organometallics* **2012**, *31* (5), 1595–1604. https://doi.org/10.1021/om201120n.

(12) Prima, D. O.; Madiyeva, M.; Burykina, J. V.; Minyaev, M. E.; Boiko, D. A.; Ananikov, V. P. Evidence for "Cocktail"-Type Catalysis in Buchwald–Hartwig Reaction. A Mechanistic Study. *Catal. Sci. Technol.* **2021**, *11* (21), 7171–7188. https://doi.org/10.1039/D1CY01601F.

(13) Valente, C.; Çalimsiz, S.; Hoi, K. H.; Mallik, D.; Sayah, M.; Organ, M. G. The Development of Bulky Palladium NHC Complexes for the Most-Challenging Cross-Coupling Reactions. *Angew. Chem. Int. Ed.* **2012**, *51* (14), 3314–3332. https://doi.org/10.1002/anie.201106131.

(14) Vanden Broeck, S. M. P.; Nahra, F.; Cazin, C. S. J. Bulky-Yet-Flexible Carbene Ligands and Their Use in Palladium Cross-Coupling. *Inorganics* **2019**, *7* (6), 78. https://doi.org/10.3390/inorganics7060078.

(15) Onoabedje, E. A.; Okoro, U. C. Ligand-Supported Palladium-Catalyzed Cross-Coupling Reactions of (Hetero) Aryl Chlorides. *Synth. Commun.* **2019**, *49* (17), 2117–2146. https://doi.org/10.1080/00397911.2019.1587778.

(16) Veerakumar, P.; Thanasekaran, P.; Lu, K.-L.; Lin, K.-C.; Rajagopal, S. Computational Studies of Versatile Heterogeneous Palladium-Catalyzed Suzuki, Heck, and Sonogashira Coupling Reactions. *ACS Sustain. Chem. Eng.* **2017**, *5* (10), 8475–8490. https://doi.org/10.1021/acssuschemeng.7b00922.

(17) Yin; Liebscher, J. Carbon−Carbon Coupling Reactions Catalyzed by Heterogeneous Palladium Catalysts. *Chem. Rev.* **2007**, *107* (1), 133–173. https://doi.org/10.1021/cr0505674.

(18) Mpungose, P. P.; Vundla, Z. P.; Maguire, G. E. M.; Friedrich, H. B. The Current Status of Heterogeneous Palladium Catalysed Heck and Suzuki Cross-Coupling Reactions. *Molecules* **2018**, *23* (7), 1676. https://doi.org/10.3390/molecules23071676.

(19) Astruc, D.; Lu, F.; Aranzaes, J. R. Nanoparticles as Recyclable Catalysts: The Frontier between Homogeneous and Heterogeneous Catalysis. *Angew. Chem. Int. Ed.* **2005**, *44* (48), 7852–7872. https://doi.org/10.1002/anie.200500766.

(20) Widegren, J. A.; Finke, R. G. A Review of the Problem of Distinguishing True Homogeneous Catalysis from Soluble or Other Metal-Particle Heterogeneous Catalysis under Reducing Conditions. *J. Mol. Catal. -Chem.* **2003**, *198* (1), 317–341. https://doi.org/10.1016/s1381-1169(02)00728-8.

(21) Crabtree, R. H. *The Organometallic Chemistry of the Transition Metals*, Seventh edition.; Wiley: Hoboken, NJ, 2019.

(22) Schmidt, A. F.; Kurokhtina, A. A. Distinguishing between the Homogeneous and Heterogeneous Mechanisms of Catalysis in the Mizoroki-Heck and Suzuki-Miyaura Reactions: Problems and Prospects. *Kinet. Catal.* **2012**, *53* (6), 714–730. https://doi.org/10.1134/s0023158412060109.

(23) Laine, R. M. Criteria for Identifying Transition Metal Cluster-Catalyzed Reactions. *J. Mol. Catal.* **1982**, *14* (2), 137–169. https://doi.org/10.1016/0304-5102(82)80034-5.

(24) Vargaftik, M. N.; Zagorodnikov, V. P.; Stolarov, I. P.; Moiseev, I. I.; Kochubey, D. I.; Likholobov, V. A.; Chuvilin, A. L.; Zamaraev, K. I. Giant Palladium Clusters as Catalysts of Oxidative Reactions of Olefins and Alcohols. *J. Mol. Catal.* **1989**, *53* (3), 315–348. https://doi.org/10.1016/0304-5102(89)80066-5.

(25) He, B.; Zhang, Y.; Liu, X.; Chen, L. In-Situ Transmission Electron Microscope Techniques for Heterogeneous Catalysis. *ChemCatChem* **2020**, *12* (7), 1853–1872. https://doi.org/10.1002/cctc.201902285.

(26) Hornstein, B. J.; Aiken, J. D.; Finke, R. G. Nanoclusters in Catalysis: A Comparison of CS2 Catalyst Poisoning of Polyoxoanion- and Tetrabutylammonium-Stabilized 40 ± 6 Å Rh(0) Nanoclusters to 5 Rh/Al2O3, Including an Analysis of the Literature Related to the CS2 to Metal Stoichiometry Issue. *Inorg. Chem.* **2002**, *41* (6), 1625–1638. https://doi.org/10.1021/ic010920y.

(27) Gonzalez-Tejuca, L.; Aika, K.; Namba, S.; Turkevich, J. Poisoning Titration Technique for Determining the Number of Active Centers in a Supported Platinum Catalyst. *J. Phys. Chem.* **1977**, *81* (14), 1399–1406. https://doi.org/10.1021/j100529a011.

(28) Crabtree, R. H. Resolving Heterogeneity Problems and Impurity Artifacts in Operationally Homogeneous Transition Metal Catalysts. *Chem. Rev.* **2012**, *112* (3), 1536–1554. https://doi.org/10.1021/cr2002905.

(29) Anton, D. R.; Crabtree, R. H. Dibenzo[a,e]Cyclooctatetraene in a Proposed Test for Heterogeneity in Catalysts Formed from Soluble Platinum-Group Metal Complexes. *Organometallics* **1983**, *2* (7), 855–859. https://doi.org/10.1021/om50001a013.

(30) Tasić, M.; Ruiz-Soriano, A.; Strand, D. Copper(I) Catalyzed Decarboxylative Synthesis of Diareno[a,e]Cyclooctatetraenes. *J. Org. Chem.* **2022**, *87* (11), 7501–7508. https://doi.org/10.1021/acs.joc.2c00286.

(31) Lin, Y.; Finke, R. G. A More General Approach to Distinguishing "Homogeneous" from "Heterogeneous" Catalysis: Discovery of Polyoxoanion- and Bu4N+-Stabilized, Isolable

and Redissolvable, High-Reactivity Ir.Apprx.190-450 Nanocluster Catalysts. *Inorg. Chem.* **1994**, *33* (22), 4891–4910. https://doi.org/10.1021/ic00100a012.

(32) Weddle, K. S.; Aiken, J. D.; Finke, R. G. Rh(0) Nanoclusters in Benzene Hydrogenation Catalysis: Kinetic and Mechanistic Evidence That a Putative [(C8H17)3NCH3]+[RhCl4]- Ion-Pair Catalyst Is Actually a Distribution of Cl- and [(C8H17)3NCH3]+ Stabilized Rh(0) Nanoclusters. *J. Am. Chem. Soc.* **1998**, *120* (23), 5653–5666. https://doi.org/10.1021/ja973045h.

(33) Sommer, W. J.; Yu, K.; Sears, J. S.; Ji, Y.; Zheng, X.; Davis, R. J.; Sherrill, C. D.; Jones, C. W.; Weck, M. Investigations into the Stability of Tethered Palladium(II) Pincer Complexes during Heck Catalysis. *Organometallics* **2005**, *24* (18), 4351–4361. https://doi.org/10.1021/om048992v.

(34) Molnár, Á. Efficient, Selective, and Recyclable Palladium Catalysts in Carbon−Carbon Coupling Reactions. *Chem. Rev.* **2011**, *111* (3), 2251–2320. https://doi.org/10.1021/cr100355b.

(35) Phan, N. T. S.; Van Der Sluys, M.; Jones, C. W. On the Nature of the Active Species in Palladium Catalyzed Mizoroki–Heck and Suzuki–Miyaura Couplings – Homogeneous or Heterogeneous Catalysis, A Critical Review. *Adv. Synth. Catal.* **2006**, *348* (6), 609–679. https://doi.org/10.1002/adsc.200505473.

(36) Chernyshev, V. M.; Astakhov, A. V.; Chikunov, I. E.; Tyurin, R. V.; Eremin, D. B.; Ranny, G. S.; Khrustalev, V. N.; Ananikov, V. P. Pd and Pt Catalyst Poisoning in the Study of Reaction Mechanisms: What Does the Mercury Test Mean for Catalysis? *ACS Catal.* **2019**, *9* (4), 2984–2995. https://doi.org/10.1021/acscatal.8b03683.

(37) Whitesides, G. M.; Hackett, Marifaith.; Brainard, R. L.; Lavalleye, J. P. P. M.; Sowinski, A. F.; Izumi, A. N.; Moore, S. S.; Brown, D. W.; Staudt, E. M. Suppression of Unwanted Heterogeneous Platinum(0)-Catalyzed Reactions by Poisoning with Mercury(0) in Systems Involving Competing Homogeneous Reactions of Soluble Organoplatinum Compounds: Thermal Decomposition of Bis(Triethylphosphine)-3,3,4,4-Tetramethylplatinacyclopentane. *Organometallics* **1985**, *4* (10), 1819–1830. https://doi.org/10.1021/om00129a023.

(38) Gorunova, O. N.; Livantsov, M. V.; Grishin, Y. K.; Ilyin, M. M.; Kochetkov, K. A.; Churakov, A. V.; Kuz'mina, L. G.; Khrustalev, V. N.; Dunina, V. V. Evidence on Palladacycle-Retaining Pathway for Suzuki Coupling. Inapplicability of Hg-Drop Test for Palladacycle Catalysed Reactions. *J. Organomet. Chem.* **2013**, *737*, 59–63. https://doi.org/10.1016/j.jorganchem.2013.03.050.

(39) Gorunova, O. N.; Novitskiy, I. M.; Grishin, Y. K.; Gloriozov, I. P.; Roznyatovsky, V. A.; Khrustalev, V. N.; Kochetkov, K. A.; Dunina, V. V. When Applying the Mercury Poisoning Test to Palladacycle-Catalyzed Reactions, One Should Not Consider the Common Misconception of Mercury(0) Selectivity. *Organometallics* **2018**, *37* (17), 2842–2858. https://doi.org/10.1021/acs.organomet.8b00363.

(40) Gorunova, O. N.; Novitskiy, I. M.; Grishin, Y. K.; Gloriozov, I. P.; Roznyatovsky, V. A.; Khrustalev, V. N.; Kochetkov, K. A.; Dunina, V. V. The Use of Control Experiments as the Sole Route to Correct the Mechanistic Interpretation of Mercury Poisoning Test Results: The Case of P,C-Palladacycle-Catalysed Reactions. *J. Organomet. Chem.* **2020**, *916*, 121245. https://doi.org/10.1016/j.jorganchem.2020.121245.

(41) Richardson, J. M.; Jones, C. W. Poly(4-Vinylpyridine) and Quadrapure TU as Selective Poisons for Soluble Catalytic Species in Palladium-Catalyzed Coupling Reactions – Application to Leaching from Polymer-Entrapped Palladium. *Adv. Synth. Catal.* **2006**, *348* (10–11), 1207–1216. https://doi.org/10.1002/adsc.200606021.

(42) Dyson, P. J. Arene Hydrogenation by Homogeneous Catalysts: Fact or Fiction? *Dalton Trans.* **2003**, No. 15, 2964–2974. https://doi.org/10.1039/B303250G.

(43) Chen, P. Electrospray Ionization Tandem Mass Spectrometry in High-Throughput Screening of Homogeneous Catalysts. *Angew. Chem. Int. Ed.* **2003**, *42* (25), 2832–2847. https://doi.org/10.1002/anie.200200560.

(44) Schröder, D. Applications of Electrospray Ionization Mass Spectrometry in Mechanistic Studies and Catalysis Research. *Acc. Chem. Res.* **2012**, *45* (9), 1521–1532. https://doi.org/10.1021/ar3000426.

(45) Zhu, W.; Yuan, Y.; Zhou, P.; Zeng, L.; Wang, H.; Tang, L.; Guo, B.; Chen, B. The Expanding Role of Electrospray Ionization Mass Spectrometry for Probing Reactive Intermediates in Solution. *Molecules* **2012**, *17* (10), 11507–11537. https://doi.org/10.3390/molecules171011507.

(46) Iacobucci, C.; Reale, S.; De Angelis, F. Elusive Reaction Intermediates in Solution Explored by ESI-MS: Reverse Periscope for Mechanistic Investigations. *Angew. Chem. Int. Ed.* **2016**, *55* (9), 2980–2993. https://doi.org/10.1002/anie.201507088.

(47) Auth, T.; Koszinowski, K.; O'Hair, R. A. J. Dissecting Transmetalation Reactions at the Molecular Level: Phenyl Transfer in Metal Borate Complexes. *Organometallics* **2020**, *39* (1), 25–33. https://doi.org/10.1021/acs.organomet.9b00521.

(48) Deuker, M.; Yang, Y.; O'Hair, R. A. J.; Koszinowski, K. Tetraorganylargentate(III) Complexes: Key Intermediates in Silver-Mediated Cross-Coupling Reactions. *Organometallics* **2021**, *40* (14), 2354–2363. https://doi.org/10.1021/acs.organomet.1c00118.

(49) O'Hair, R. A. J. Organometallic Gas-Phase Ion Chemistry and Catalysis: Insights into the Use of Metal Catalysts to Promote Selectivity in the Reactions of Carboxylic Acids and Their Derivatives. *Mass Spectrom. Rev.* **2021**, *40* (6), 782–810. https://doi.org/10.1002/mas.21654.

(50) Thomas, G. T.; Ronda, K.; McIndoe, J. S. A Mechanistic Investigation of the Pd-Catalyzed Cross-Coupling between N-Tosylhydrazones and Aryl Halides. *Dalton Trans.* **2021**, *50* (43), 15533–15537. https://doi.org/10.1039/D1DT03161A.

(51) Ting, M. Y. C.; Yunker, L. P. E.; Chagunda, I. C.; Hatlelid, K.; Vieweg, M.; McIndoe, J. S. A Mechanistic Investigation of the Suzuki Polycondensation Reaction Using MS/MS Methods. *Catal. Sci. Technol.* **2021**. https://doi.org/10.1039/D1CY00743B.

(52) Joshi, A.; Zijlstra, H. S.; Collins, S.; McIndoe, J. S. Catalyst Deactivation Processes during 1-Hexene Polymerization. *ACS Catal.* **2020**, *10* (13), 7195–7206. https://doi.org/10.1021/acscatal.0c01607.

(53) Bütikofer, A.; Chen, P. Cyclopentadienone Iron Complex-Catalyzed Hydrogenation of Ketones: An Operando Spectrometric Study Using Pressurized Sample Infusion-Electrospray Ionization-Mass Spectrometry. *Organometallics* **2022**, *41* (16), 2349–2364. https://doi.org/10.1021/acs.organomet.2c00341.

(54) Thomas, G. T.; Donnecke, S.; Chagunda, I. C.; McIndoe, J. S. Pressurized Sample Infusion. *Chemistry–Methods* **2022**, *2* (1). https://doi.org/10.1002/cmtd.202100068.

(55) Baier, H.; Kelling, A.; Holdt, H.-J. PEPPSI-Effect on Suzuki–Miyaura Reactions Using 4,5-Dicyano-1,3-Dimesitylimidazol-2-Ylidene-Palladium Complexes: A Comparison between Trans-Ligands. *Eur. J. Inorg. Chem.* **2015**, *2015* (11), 1950–1957. https://doi.org/10.1002/ejic.201500010.

(56) Baier, H.; Kelling, A.; Schilde, U.; Holdt, H.-J. Investigation of the Catalytic Activity of a 2-Phenylidenepyridine Palladium(II) Complex Bearing 4,5-Dicyano-1,3-Bis(Mesityl)Imidazol-2-Ylidene in the Mizoroki-Heck Reaction. *Z. Für Anorg. Allg. Chem.* **2016**, *642* (2), 140–147. https://doi.org/10.1002/zaac.201500625.

(57) Vikse, K. L.; Henderson, M. A.; Oliver, A. G.; McIndoe, J. S. Direct Observation of Key Intermediates by Negative-Ion Electrospray Ionisation Mass Spectrometry in Palladium-Catalysed Cross-Coupling. *Chem. Commun.* **2010**, *46* (39), 7412–7414. https://doi.org/10.1039/C0CC02773A.

(58) Weber, P.; Biafora, A.; Doppiu, A.; Bongard, H.-J.; Kelm, H.; Gooßen, L. J. A Comparative Study of Dibenzylideneacetone Palladium Complexes in Catalysis. *Org. Process Res. Dev.* **2019**, *23* (7), 1462–1470. https://doi.org/10.1021/acs.oprd.9b00214.

(59) Janusson, E.; Zijlstra, H. S.; Nguyen, P. P. T.; MacGillivray, L.; Martelino, J.; McIndoe, J. S. Real-Time Analysis of Pd2(Dba)3 Activation by Phosphine Ligands. *Chem. Commun.* **2017**, *53* (5), 854–856. https://doi.org/10.1039/C6CC08824D.

(60) Barański, A.; Kryska, A.; Galus, Z. On the Electrochemical Properties of the Pd + Hg System. *J. Electroanal. Chem.* **1993**, *349* (1), 341–354. https://doi.org/10.1016/0022-0728(93)80183-I.

(61) Ji, Y.; Plata, R. E.; Regens, C. S.; Hay, M.; Schmidt, M.; Razler, T.; Qiu, Y.; Geng, P.; Hsiao, Y.; Rosner, T.; Eastgate, M. D.; Blackmond, D. G. Mono-Oxidation of Bidentate Bis-Phosphines in Catalyst Activation: Kinetic and Mechanistic Studies of a Pd/Xantphos-Catalyzed C–H Functionalization. *J. Am. Chem. Soc.* **2015**, *137* (41), 13272–13281. https://doi.org/10.1021/jacs.5b01913.

(62) Tereniak, S. J.; Landis, C. R.; Stahl, S. S. Are Phosphines Viable Ligands for Pd-Catalyzed Aerobic Oxidation Reactions? Contrasting Insights from a Survey of Six Reactions. *ACS Catal.* **2018**, *8* (4), 3708–3714. https://doi.org/10.1021/acscatal.8b01009.

(63) Hesketh, A. V.; Nowicki, S.; Baxter, K.; Stoddard, R. L.; McIndoe, J. S. Simplified Real-Time Mass Spectrometric Analysis of Reactions. *Organometallics* **2015**, *34* (15), 3816–3819. https://doi.org/10.1021/acs.organomet.5b00460.

(64) Yunker, L. P. E.; Ahmadi, Z.; Logan, J. R.; Wu, W.; Li, T.; Martindale, A.; Oliver, A. G.; McIndoe, J. S. Real-Time Mass Spectrometric Investigations into the Mechanism of the Suzuki–Miyaura Reaction. *Organometallics* **2018**, *37* (22), 4297–4308. https://doi.org/10.1021/acs.organomet.8b00705.

(65) Omari, I.; Randhawa, P.; Randhawa, J.; Yu, J.; McIndoe, J. S. Structure, Anion, and Solvent Effects on Cation Response in ESI-MS. *J. Am. Soc. Mass Spectrom.* **2019**, *30* (9), 1750–1757. https://doi.org/10.1007/s13361-019-02252-0.

(66) de Magalhães, M. E. A.; Tubino, M. A Possible Path for Mercury in Biological Systems: The Oxidation of Metallic Mercury by Molecular Oxygen in Aqueous Solutions. *Sci. Total Environ.* **1995**, *170* (3), 229–239. https://doi.org/10.1016/0048-9697(95)04711-5.

(67) Amyot, M.; Morel, F. M. M.; Ariya, P. A. Dark Oxidation of Dissolved and Liquid Elemental Mercury in Aquatic Environments. *Environ. Sci. Technol.* **2005**, *39* (1), 110–114. https://doi.org/10.1021/es035444k.

(68) Hocsman, A.; Di Nezio, S.; Charlet, L.; Avena, M. On the Mechanisms of Dissolution of Montroydite [HgO(s)]: Dependence of the Dissolution Rate on PH, Temperature, and Stirring Rate. *J. Colloid Interface Sci.* **2006**, *297* (2), 696–704. https://doi.org/10.1016/j.jcis.2005.11.020.

(69) Amini, M. K.; Ghaedi, M.; Rafi, A.; Habibi, M. H.; Zohory, M. M. Iodide Selective Electrodes Based on Bis(2-Mercaptobenzothiazolato) Mercury(II) and Bis(4-Chlorothiophenolato) Mercury(II) Carriers. *Sensors* **2003**, *3* (11), 509–523. https://doi.org/10.3390/s31100509.

(70) Butcher, C. P. G.; Johnson, B. F. G.; McIndoe, J. S.; Yang, X.; Wang, X.-B.; Wang, L.-S. Collision-Induced Dissociation and Photodetachment of Singly and Doubly Charged Anionic Polynuclear Transition Metal Carbonyl Clusters: Ru3Co(CO)13−, Ru6C(CO)162−, and Ru6(CO)182−. *J. Chem. Phys.* **2002**, *116* (15), 6560–6566. https://doi.org/10.1063/1.1462579.

(71) Bumagin, N. A.; More, P. G.; Beletskaya, I. P. Palladium-Catalyzed Cross-Coupling Reactions of Organomercurials with Organic Halides. *J. Organomet. Chem.* **1989**, *364* (1), 231–234. https://doi.org/10.1016/0022-328X(89)85346-X.

(72) Bumagin, N. A.; Kalinovskii, I. O.; Beletskaya, I. P. Arylation of Heterocycles in the Reaction of Heterocyclic Mercury Derivatives in the Presence of Palladium Complexes. *Chem. Heterocycl. Compd.* **1983**, *19* (11), 1159–1162. https://doi.org/10.1007/BF00515346.

(73) Bumagin, N. A.; Kalinovskii, I. O.; Beletskaya, I. P. Synthesis of Symmetrical Diaryl Ketones by Carbonylation of Organomercury Compounds in the Presence of Palladium and Rhodium Complexes. *Bull. Acad. Sci. USSR Div. Chem. Sci.* **1982**, *31* (1), 211–211. https://doi.org/10.1007/BF00954452.

(74) Beletskaya, I. P. The Cross-Coupling Reactions of Organic Halides with Organic Derivatives of Tin, Mercury and Copper Catalyzed by Palladium. *J. Organomet. Chem.* **1983**, *250* (1), 551–564. https://doi.org/10.1016/0022-328X(83)85077-3.

(75) Bumagin, N. A.; Kalinovskii, I. O.; Beletskaya, I. P. Reactions of Organometallic Compounds Catalyzed by Transition Metal Complexes. Communication 6. Reactions of Organomercury Compounds with Acid Chlorides in the Presence of Palladium, Nickel, and Rhodium Complexes. *Bull. Acad. Sci. USSR Div. Chem. Sci.* **1984**, *33* (10), 2144–2149. https://doi.org/10.1007/BF00954101.

(76) Tsvetkov, A. V.; Latyshev, G. V.; Lukashev, N. V.; Beletskaya, I. P. Palladium-Catalyzed Cross-Coupling Reaction of Bis(Ferrocenyl)Mercury with Aryl Iodides. *Tetrahedron Lett.* **2000**, *41* (20), 3987–3990. https://doi.org/10.1016/S0040-4039(00)00535-9.

(77) Beletskaya, I. P.; Tsvetkov, A. V.; Latyshev, G. V.; Tafeenko, V. A.; Lukashev, N. V. Bis(Ferrocenyl)Mercury as a Source of Ferrocenyl Moiety in Pd-Catalyzed Reactions of Carbon–Carbon Bond Formation. *J. Organomet. Chem.* **2001**, *637–639*, 653–663. https://doi.org/10.1016/S0022-328X(01)00979-2.

(78) Rasmussen, S. C. Transmetalation: A Fundamental Organometallic Reaction Critical to Synthesis and Catalysis. *ChemTexts* **2020**, *7* (1), 1. https://doi.org/10.1007/s40828-020-00124-9.

(79) Gubin, S. P.; Rubezhov, A. Z.; Denisovich, L. I.; Nesmeyanov, A. N. Reaction of Metallic Mercury with π-Allyl Compounds of Palladium. *Bull. Acad. Sci. USSR Div. Chem. Sci.* **1966**, *15* (9), 1630–1630. https://doi.org/10.1007/BF00848943.

(80) Nesmeyanov, A. N.; Rubezhov, A. Z.; Leites, L. A.; Gubin, S. P. The Reactions of Metallic Mercury with π-Allyl Compounds of Ni, Pd and Pt. *J. Organomet. Chem.* **1968**, *12* (1), 187–198. https://doi.org/10.1016/S0022-328X(00)90912-4.

(81) Harvey, P. D.; Aye, K. T.; Hierso, K.; Isabel, E.; Lognot, I.; Mugnier, Y.; Rochon, F. D. Electron-Ligand Interchange Reactions between Palladium(II) Complexes and Mercury and Single-Crystal X-Ray Characterization of the D10-D10 Binuclear [Hg2(Dppm)2Cl3]Cl Complex. *Inorg. Chem.* **1994**, *33* (26), 5981–5982. https://doi.org/10.1021/ic00104a002.

(82) Henderson, W.; McIndoe, J. S. *Mass Spectrometry of Inorganic and Organometallic Compounds*; John Wiley & Sons, Ltd.: New York, 2005.

(83) Garrou, P. E. Transition-Metal-Mediated Phosphorus-Carbon Bond Cleavage and Its Relevance to Homogeneous Catalyst Deactivation. *Chem. Rev.* **1985**, *85* (3), 171–185. https://doi.org/10.1021/cr00067a001.

(84) Alcazar-Roman, L. M.; Hartwig, J. F.; Rheingold, A. L.; Liable-Sands, L. M.; Guzei, I. A. Mechanistic Studies of the Palladium-Catalyzed Amination of Aryl Halides and the Oxidative Addition of Aryl Bromides to Pd(BINAP)2 and Pd(DPPF)2: An Unusual Case of Zero-Order Kinetic Behavior and Product Inhibition. *J. Am. Chem. Soc.* **2000**, *122* (19), 4618–4630. https://doi.org/10.1021/ja9944599.

(85) Fiebig, L.; Schlörer, N.; Schmalz, H.-G.; Schäfer, M. Aryl–Phenyl Scrambling in Intermediate Organopalladium Complexes: A Gas-Phase Study of the Mizoroki–Heck Reaction. *Chem. – Eur. J.* **2014**, *20* (17), 4906–4910. https://doi.org/10.1002/chem.201400115.

(86) Lee, Y. H.; Morandi, B. Transition Metal-Mediated Metathesis between P–C and M–C Bonds: Beyond a Side Reaction. *Coord. Chem. Rev.* **2019**, *386*, 96–118. https://doi.org/10.1016/j.ccr.2018.12.001.

(87) Agrawal, D.; Zins, E.-L.; Schröder, D. Intramolecular Scrambling of Aryl Groups in Organopalladium Complexes [ArPd(PPh3)2]+: From Solution to the Gas Phase, Back Again, and In-Between. *Chem. – Asian J.* **2010**, *5* (7), 1667–1676. https://doi.org/10.1002/asia.201000086.

(88) Segelstein, B. E.; Butler, T. W.; Chenard, B. L. Equilibration of the Oxidative Addition Product of Tetrakis(Triphenylphosphine)Palladium and Electron-Rich Aryl Halides Leads to Product Scrambling in the Stille Reaction. *J. Org. Chem.* **1995**, *60* (1), 12–13. https://doi.org/10.1021/jo00106a006.

(89) Sakamoto, M.; Shimizu, I.; Yamamoto, A. Palladium-Catalyzed Cleavage of P-C Bonds in Quaternary Phosphonium Salts and Its Applications to Organic Synthesis. *Chem. Lett.* **1995**, *24* (12), 1101–1102. https://doi.org/10.1246/cl.1995.1101.

(90) Wu, S.-Q.; Zhang, S.-Q.; Hong, X. Understanding the Mechanism and Reactivity of Pd-Catalyzed C–P Bond Metathesis of Aryl Phosphines: A Computational Study. *Org. Biomol. Chem.* **2020**, *18* (28), 5414–5419. https://doi.org/10.1039/D0OB00719F.

(91) Zocher, E.; Sigrist, R.; Chen, P. Threshold CID Investigation of Isomeric Cu(I) Azabox Complexes. *Inorg. Chem.* **2007**, *46* (26), 11366–11370. https://doi.org/10.1021/ic701688t.

(92) Armentrout, P. B. Threshold Collision-Induced Dissociations for the Determination of Accurate Gas-Phase Binding Energies and Reaction Barriers. In *Modern Mass Spectrometry*; Schalley, C. A., Ed.; Topics in Current Chemistry; Springer: Berlin, Heidelberg, 2003; pp 233–262. https://doi.org/10.1007/3-540-36113-8_7.

(93) Shuman, N. S.; Ard, S. G.; Sweeny, B. C.; Viggiano, A. A.; Owen, C. J.; Armentrout, P. B. Methane Adducts of Gold Dimer Cations: Thermochemistry and Structure from Collision-Induced Dissociation and Association Kinetics. *J. Phys. Chem. A* **2020**, *124* (17), 3335–3346. https://doi.org/10.1021/acs.jpca.0c01217.

(94) Zhang, R.; Li, P.-P.; Gu, G.-G.; Ren, W.-M. Evaluation of the Lewis Acidity of Metal Complexes Using ESI Mass Spectrometry. *Eur. J. Mass Spectrom.* **2020**, *26* (5), 332–340. https://doi.org/10.1177/1469066720944330.